










A supersonic laser ablation beam source with narrow velocity spreads

Cite as: Rev. Sci. Instrum. **92**, 033202 (2021); <https://doi.org/10.1063/5.0035568>

Submitted: 03 November 2020 . Accepted: 06 February 2021 . Published Online: 03 March 2021

 P. Aggarwal,  H. L. Bethlem, A. Boeschoten,  A. Borschevsky, K. Esajas,  Y. Hao,  S. Hoekstra,  K. Jungmann,  V. R. Marshall, T. B. Meijknecht, M. C. Mooij, R. G. E. Timmermans, A. Touwen,  W. Ubachs,  L. Willmann, Y. Yin, and A. Zapara



View Online



Export Citation



CrossMark

ARTICLES YOU MAY BE INTERESTED IN

[High frame rate emission spectroscopy for ablation tests in plasma wind tunnel](#)



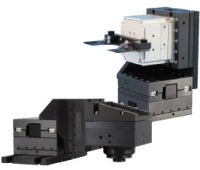
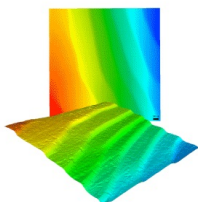
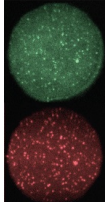
Review of Scientific Instruments **92**, 033101 (2021); <https://doi.org/10.1063/5.0040801>

[Characterization of micrometer-size laser beam using a vibrating wire as a miniature scanner](#)

Review of Scientific Instruments **92**, 033303 (2021); <https://doi.org/10.1063/5.0028666>

[Incoherent Thomson scattering system for PHase space MApping \(PHASMA\) experiment](#)

Review of Scientific Instruments **92**, 033102 (2021); <https://doi.org/10.1063/5.0040606>

 MCL MAD CITY LABS INC. www.madcitylabs.com	<p>Nanopositioning Systems</p> 	<p>Modular Motion Control</p> 	<p>AFM and NSOM Instruments</p> 	<p>Single Molecule Microscopes</p> 
---	--	--	---	--

A supersonic laser ablation beam source with narrow velocity spreads

Cite as: *Rev. Sci. Instrum.* **92**, 033202 (2021); doi: [10.1063/5.0035568](https://doi.org/10.1063/5.0035568)

Submitted: 3 November 2020 • Accepted: 6 February 2021 •

Published Online: 3 March 2021

















View Online



Export Citation



CrossMark

P. Aggarwal,^{1,2}  H. L. Bethlem,^{1,3}  A. Boeschoten,^{1,2}  A. Borschevsky,^{1,2}  K. Esajas,^{1,2}  Y. Hao,^{1,2} 
S. Hoekstra,^{1,2,a)}  K. Jungmann,^{1,2}  V. R. Marshall,^{1,2}  T. B. Meijknecht,^{1,2}  M. C. Mooij,^{2,3}  R. G. E. Timmermans,^{1,2}
A. Touwen,^{1,2}  W. Ubachs,³  L. Willmann,^{1,2}  Y. Yin,^{1,2} and A. Zapara^{1,2}

AFFILIATIONS

¹Van Swinderen Institute for Particle Physics and Gravity, University of Groningen, Zernikelaan 25 9747AA, The Netherlands

²Nikhef, National Institute for Subatomic Physics, Science Park 105, 1098 XG Amsterdam, The Netherlands

³Department of Physics and Astronomy, and LaserLaB, Vrije Universiteit Amsterdam, De Boelelaan 1081, 1081 HV Amsterdam, The Netherlands

^{a)} Author to whom correspondence should be addressed: s.hoekstra@rug.nl

ABSTRACT

A supersonic beam source for SrF and BaF molecules is constructed by combining the expansion of carrier gas (a mixture of 2% SF₆ and 98% argon) from an Even–Lavie valve with laser ablation of a barium/strontium metal target at a repetition rate of 10 Hz. Molecular beams with a narrow translational velocity spread are produced at relative values of $\Delta v/v = 0.053(11)$ and $0.054(9)$ for SrF and BaF, respectively. The relative velocity spread of the beams produced in our source is lower in comparison with the results from other metal fluoride beams produced in supersonic laser ablation sources. The rotational temperature of BaF is measured to be 3.5 K. The source produces 6×10^8 and 10^7 molecules per steradian per pulse in the $X^2\Sigma^+$ ($v = 0, N = 1$) state of BaF and SrF molecules, respectively, a state amenable to Stark deceleration and laser cooling.

© 2021 Author(s). All article content, except where otherwise noted, is licensed under a Creative Commons Attribution (CC BY) license (<http://creativecommons.org/licenses/by/4.0/>). <https://doi.org/10.1063/5.0035568>

I. INTRODUCTION

Supersonic expansion is a proven method to produce beams of molecules with a small velocity spread and low translational and rotational temperatures, resulting in relatively high population of the lowest energy states.^{1,2} A small velocity spread is desirable for high-resolution spectroscopy,^{3–5} for collision experiments,^{6,7} and also for efficient deceleration of molecules in a Stark decelerator.^{8–10} This is because it reduces Doppler broadening, ensures good resolution of the collision energy in collision experiments, and facilitates good phase-space matching at the entrance of the Stark decelerator.

The smallest relative velocity spread and lowest temperatures have been achieved in the expansion of helium through a pulsed nozzle at high pressures.¹¹ Beams of stable molecules were produced by expansion of molecules seeded in light carrier gases such as beams of nitric oxide and aniline seeded in helium^{12,13} with rotational temperatures of order 1 K. The coldest translational temperatures can

be achieved when the seeded molecules completely thermalize with the carrier gas. However, for the production of some molecular species, laser ablation is needed, which sometimes leads to a larger velocity spread.¹⁴ The ablation technique was originally used to generate clusters of atoms where a high-energy laser beam vaporizes the material of interest, which is then entrained in a supersonically expanding gas flow.^{15–17} Later, metal-atom beams were produced, in which the products of laser ablation of the corresponding solid target were entrained in neutral gases expanding supersonically from pulsed valves for crossed beam experiments.^{18–20} Beams of metal compounds are now also produced through the reactions of ablation products with impurity gases added to the carrier gas. For example, beams of SrF,²¹ CoF,²² YF,²³ YbF,²⁴ HfF⁺,²⁵ and BaF^{14,26} were produced by adding SF₆ as an impurity gas.

In the present study, a combination of an Even–Lavie valve²⁷ with laser ablation is presented. Such a valve can produce short ($\sim 25 \mu\text{s}$) and dense pulses with relatively low operating currents in

comparison with other valves, which prevents the heating of the gas pulse. It can also be operated at high backing pressures, which leads to a large pressure gradient, thereby reducing the kinetic temperature of the gas pulse. Such a combination has previously been used to produce beams to study reaction dynamics^{28,29} and collision experiments between atoms and molecules in a magnetic and a static quadrupole trap.^{30,31} Droplets of helium have also been produced by expansion through a pulsed Even–Lavie valve to which lithium atoms are doped by ablation.³² This combination has been used here for the production of supersonic beams of two alkaline-earth metal fluorides, SrF and BaF. These relatively heavy molecules are considered as target probes to test fundamental symmetry violation beyond the Standard Model.^{33,34} We demonstrate the small velocity spread of the produced beams of SrF and BaF and compare our results with other ablation sources for metal fluorides.^{14,24,26}

II. CONSTRUCTION

Our experimental setup for the production of molecules is shown in Fig. 1. An Even–Lavie valve creates pulses of carrier gas argon seeded with 2% SF₆ with the gate length set to ~35 μs. The metal of interest, in our case barium or strontium, is mounted in the form of a 3 mm thick disk with a diameter of 56 mm inside a vacuum chamber at a distance of 4 mm along the line of expansion and 5 mm in the direction transverse to the beam. The transverse distance of 5 mm has been optimized to obtain maximum molecular flux, with the beam collapsing for a distance less than 2 mm. The target was rotated with a vacuum compatible Picomotor actuator with a rotating shaft (Newport 8341-V). Laser light pulses of 10 ns length, 20 mJ energy, and 4 mm spot size, at a wavelength of 532 nm, from a Nd:YAG laser ablate the metal target at the 3 mm thick surface of the disk. The spot size of the ablation pulse is slightly larger than the maximum 3 mm wide region on the side of the target disk, which can be ablated. The ablation products are entrained in the expanding carrier gas. The molecules formed are thermalized by undergoing collisions with the corresponding noble gas atoms. A skimmer of 5 mm diameter (Beam Dynamics, model 2) mounted at a distance of 28 cm from the exit of the valve selects

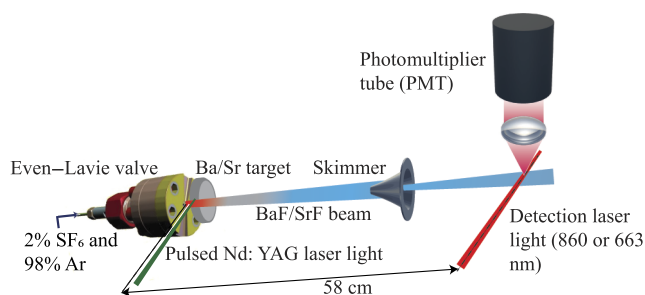


FIG. 1. Experimental setup of the supersonic source. An Even–Lavie valve produces short pulses of carrier gas consisting of 98% Ar and 2% SF₆. A high-energy Nd:YAG laser light pulse ablates the metal of interest, which is then entrained in the supersonically expanding carrier gas. The molecules in the $X^2\Sigma^+$ ($v = 0$, $N = 1$) state are detected by laser-induced fluorescence light, which is collected on a photo-multiplier tube cathode. Only the collection lens is shown in the figure.

the central part of the beam. The molecules are detected 58 cm downstream of the valve exit. This source is operated at a repetition rate of 10 Hz.

In the detection chamber, the molecules SrF and BaF are detected by laser-induced fluorescence (LIF) by exciting the molecules from the ground electronic state $X^2\Sigma^+$ ($v = 0$, $N = 1$) to the first electronically excited state $A^2\Pi_{1/2}$ ($v = 0$, $J = 1/2$) by light from a diode laser at a wavelength of 663 nm for SrF detection and by light from a Ti:sapphire laser at a wavelength of 860 nm for BaF detection, respectively. The hyperfine levels in the ground state of SrF are approximately covered by frequency sidebands to the laser light frequency, which were created by passing the laser light through an electro-optic modulator driven by a sinusoidal signal of 42.5 MHz frequency and at a modulation index of 2.6. For the detection of BaF, we did not use frequency sidebands; therefore, the hyperfine structure in the ground state of BaF is not covered and the detection laser is tuned to the strongest signal when probing the $N = 1$ level. The fluorescence emitted by BaF and SrF molecules is collected by using a 2-in. achromatic lens of 75 mm focal length (65.7 mm back focal length) in the upward direction and 1-in. achromatic lens of 35 mm focal length (27.3 mm back focal length) in the upward and downward directions, respectively. The 663 nm wavelength light is further imaged with a 1-in. biconvex lens of 60 mm focal length onto the photomultiplier tube (PMT) with a quantum efficiency of 0.39 with the total magnification of the entire lens assembly equal to 1.7. The 860 nm wavelength light is imaged onto the PMT with a quantum efficiency of 0.13, using a 2-in. achromatic lens and a 1-in. biconvex lens of 25.4 mm focal length with the total magnification of the entire lens assembly equal to 0.5. A narrow bandpass filter with transmission of 99% (60%) at the wavelength of 663(10) nm [860(10) nm] is placed in front of the PMT to discriminate the fluorescence photons corresponding to the exciting transition from background room light. The detection chamber is blackened inside with paint (AZ Technology MLS-85-HB) to reduce the background counts from scattered laser light. The chamber contains copper aperture rings with a knife edge along their inside diameter in the detection laser light path to avoid scattering of light.

III. RESULTS

A. Time-of-flight profile

The voltage pulses from the PMT are processed in a single-pulse discriminator. They are further sent to a time-to-digital converter (TDC). The TDC records time stamps for the input voltage signal pulses with resolution below 1 ns.³⁵ The time-of-flight (TOF) profiles for SrF and BaF molecules taken at a backing pressure of 8 bars are shown in Fig. 2 (black dotted line).

The time-of-flight profile is shown over the time frame of 700 μs–1250 μs with a bin size of 5 μs where $t = 0$ corresponds to the time of ablation of the metal target with the pulsed Nd:YAG laser operating at a repetition rate of 10 Hz. The arrival time of the SrF and BaF molecular beams is 983(7) μs and 951(6) μs, respectively.

The velocity distribution of the molecules with central velocity v_0 and with longitudinal velocities in the interval v to $v + dv$ can be expressed as

$$f(v) dv = Av^3 \exp(-m(v - v_0)^2 / 2k_B T) dv, \quad (1)$$

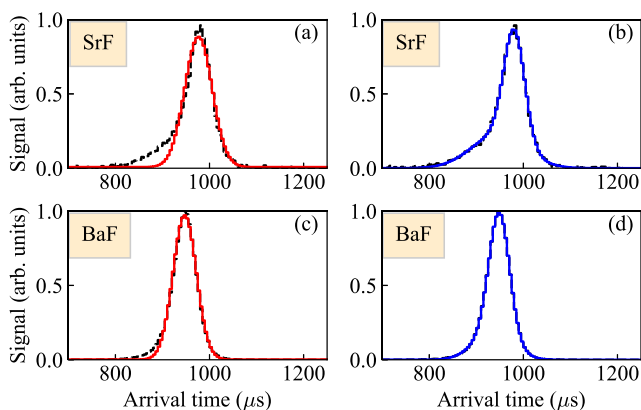


FIG. 2. Time-of-flight profile of SrF [(a) and (b)] and BaF [(c) and (d)] molecular beams at a backing pressure of 8 bars obtained by laser-induced fluorescence (LIF) detection on the transition $A^2\Pi_{1/2} (\nu = 0, J = 1/2) \leftarrow X^2\Sigma^+ (\nu = 0, N = 1)$ shown with a black dotted line. The red solid line depicts a single Gaussian profile fitted to the data, and the blue solid line depicts a fit with two Gaussian profiles. The SrF and BaF molecules travel a distance of 58.0 cm in an average time of 983(7) μs and 951(6) μs , respectively.

where A is a normalization constant, m is the mass of the molecule, and T is the translational temperature.^{36,37} Distribution (1) can be converted to a time-of-flight (TOF) distribution by substituting $t = L/v$ and $t_0 = L/v_0$,

$$g(t) dt = \frac{CL^4}{t^5} \exp\left(-\frac{mL^2}{2k_B T} \left(\frac{t-t_0}{t_0}\right)^2\right) dt. \quad (2)$$

Here, we take into account that the molecules start from a very short pulse. The above distribution resembles a Gaussian profile on using the approximation, $t \approx t_0$,

$$g(t) dt = \frac{CL^4}{t_0^4} \exp\left(-\frac{mL^2}{2k_B T} \frac{(t-t_0)^2}{t_0^4}\right) dt. \quad (3)$$

Therefore, fitting a Gaussian profile to the time-of-flight profile is a heuristic way of approximating the data to extract the properties of the beam. The result of a single Gaussian shape to the data is shown by red solid lines in Figs. 2(a) and 2(c). Apparently, a single Gaussian does not describe all the data, notably for SrF, which has excess signal counts at the leading edge of the TOF profile. This is observed mostly for higher backing pressure conditions in the case of SrF, and we interpret that it is a part of the molecular beam that is not well thermalized with the carrier gas. To quantify the non-thermalized part, we fit two Gaussian profiles to our TOF profile [shown by blue solid lines in Figs. 2(b) and 2(d)]. The broader pedestals under the narrower TOF peaks contain 43% and 29% of the observed molecules for SrF and BaF, respectively (see Fig. 2).

In Fig. 3, we fit two Gaussian profiles to SrF and BaF time-of-flight profiles at different backing pressures. The reduced χ^2 , where two Gaussian profiles are used, of the 14 fits in Fig. 3 vary between 0.90 and 1.17. The broader pedestal under the main peak contributes

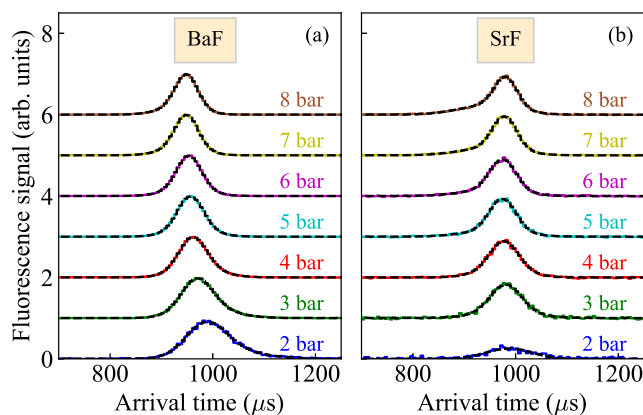


FIG. 3. Time-of-flight profiles of BaF [panel (a)] and SrF [panel (b)] molecular beams at different backing pressures in the range of 2 bars–8 bars obtained by laser-induced fluorescence detection on the transition $A^2\Pi_{1/2} (\nu = 0, J = 1/2) \leftarrow X^2\Sigma^+ (\nu = 0, N = 1)$. The black dotted line on the top depicts the two Gaussian fits to the time-of-flight profiles of BaF and SrF. A vertical offset has been added to the subsequent time-of-flight profiles for the sake of clarity.

between 26% and 43% to the arrival-time histogram of SrF with its contribution increasing with higher backing pressure. The broader pedestal contributes 25%–31% to the time-of-flight histogram of BaF without any specific trend with the backing pressure.

The further analysis is based only on the narrow feature of the time-of-flight profile.

B. Relative velocity spread

The velocity of SrF and BaF molecular beams is calculated to be 590(4) m/s and 610(4) m/s, respectively. The time-spread (FWHM) of the time-of-flight profile of SrF and BaF is given by $2\sqrt{2\ln(2)}\sigma$, where σ is the width of the Gaussian fit. The time variances of the SrF and BaF beams at a backing pressure of 8 bars are calculated to be 52.4(5) μs and 51.2(4) μs , respectively. The corresponding velocity spread Δv is calculated to be 31.5(3) m/s and 32.9(2) m/s for SrF and BaF, respectively, by assuming that the molecules start from a very short pulse, and hence, $v = L/t$. The relative velocity spread $\Delta v/v$ is a representation of the cooling process and gives a measure of the translational degrees of freedom. We compare our relative velocity values with those obtained in other supersonic beam sources for metal fluorides in Table II. Using $\Delta v = \sqrt{8kT \ln 2/m}$,³⁸ the translational temperature of SrF and BaF is calculated to be 2.3(1) K and 5.2(1) K, respectively.

The typical velocity of argon in a supersonic expansion from an Even–Lavie valve at room temperature is 570 m/s with a small velocity spread of 56 m/s at 5 bars backing pressure.^{39,40} The velocity spread of the two molecular beams, SrF and BaF, with argon as the carrier gas at 5 bars backing pressure is 36.8(6) m/s and 37.2(2) m/s, respectively. The velocity spread of BaF and SrF is very similar despite the fact that the mass of BaF is 1.46 times higher than that of SrF. This means that the velocity of the molecular beams appears to be determined completely by the thermalization process by the carrier gas.

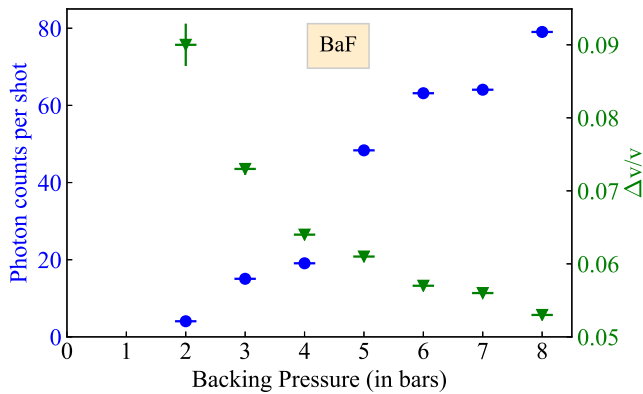


FIG. 4. Average photon counts detected per shot on exciting the BaF molecules on the transition $A^2\Pi_{1/2}(\nu = 0, J = 1/2) \leftarrow X^2\Sigma^+(\nu = 0, N = 1)$ (blue circles) and the relative velocity spread (green triangles) as a function of backing pressure.

C. Backing pressure variation

The relative velocity spread of the molecular beam typically depends strongly on the backing pressure. This is studied by varying the backing pressure from 2 bars to 8 bars, as shown in Figs. 4 and 5. The average photon counts per shot, which is defined as the difference of signal counts and background counts divided by the total number of shots, increases with increasing backing pressure both for SrF and BaF up to 8 bars, which is the maximum pressure applied to our gas supply line. The increase in the photon counts per pulse with increased backing pressure is due to an increase in the number of BaF and SrF molecules. The increase in the BaF and SrF molecules can, in turn, be attributed to an increase in the barium and strontium atoms, respectively, entrained in the carrier gas flow at the high backing pressures. The velocity spread of the BaF beam Δv reduces to the minimum value of 32.9(2) m/s corresponding to a relative velocity spread $\Delta v/v$ of 0.054(9) at a backing pressure of 8 bars. The relative velocity spread for SrF is also lowest at our applied highest backing pressure of 8 bars, with a velocity spread and relative velocity spread of 31.5(3) m/s and 0.053(11) m/s, respectively.

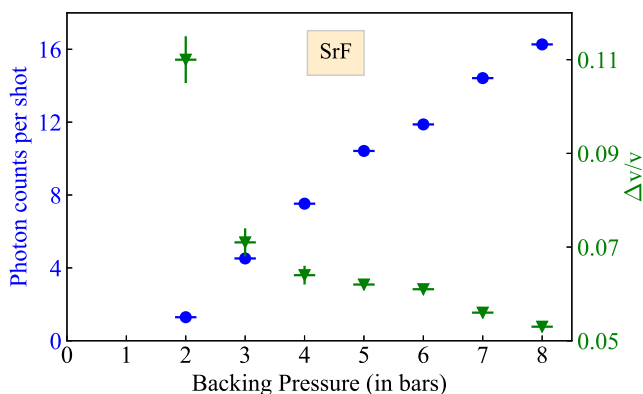


FIG. 5. Average photon counts detected per shot on exciting the SrF molecules on the transition $A^2\Pi_{1/2}(\nu = 0, J = 1/2) \leftarrow X^2\Sigma^+(\nu = 0, N = 1)$ (blue circles) and the relative velocity spread (green triangles) as a function of backing pressure.

D. Rotational temperature

The rotational spectrum for the transition from the lowest rotational levels of the $X^2\Sigma^+(\nu = 0)$ state to the first electronically excited state $A^2\Pi_{1/2}(\nu = 0)$ in BaF is obtained by scanning the laser frequency from (11 630.38–11 631.00) cm^{-1} (Fig. 6). The spectrum taken at a backing pressure of 7 bars is the upper trace, and the stick spectrum below is simulated by the program PGOPHER⁴¹ using the molecular constants of the $A^2\Pi_{1/2}$ state.^{5,42} The simulated spectrum corresponds to a rotational temperature of 3.5 K, and it is similar in the intensity ratios of the rotational levels to the experimental spectrum. The highest molecular population is in the $N = 1$ rotational state.

E. Number of molecules

The number of molecules in the beam after the skimmer can be estimated using the following formula:

$$N = \frac{S}{QE \times T \times (\Omega/4\pi) \times n} \times \frac{\pi \times (\Delta y/2)^2}{w \times \Delta y} \times \frac{M \times \Delta y}{a}, \quad (4)$$

where S is the maximum signal photon counts per shot detected by the PMT, QE is the quantum efficiency of the PMT at the specific wavelength, T is the transmission of the fluorescence collection lenses and filter, Ω is the collection solid angle, and n corresponds to the average number of photons that are scattered by a single molecule calculated from the hyperfine branching ratios.^{43,44} The second term in the multiplication denotes the fraction of molecules detected by the laser beam in the transverse direction where Δy is the transverse spread of the molecule beam and w is the spot size of the detection laser beam. The third term in the multiplication takes into account the fraction of the fluorescence imaged onto the active area of the PMT, where M is the magnification of the collection optics and $a = 5$ mm is the size of the active area of the PMT. All these parameters for the detection of SrF and BaF beams are specified in Table I.

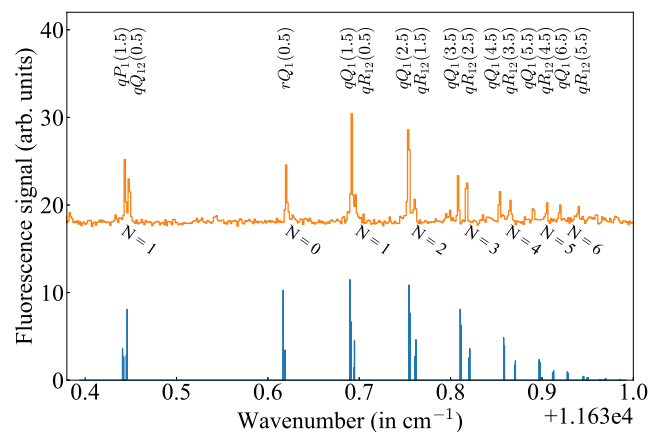


FIG. 6. Rotational spectrum for the transition from $X^2\Sigma^+(\nu = 0)$ to $A^2\Pi_{1/2}(\nu = 0)$ state in BaF. An offset is added to the upper trace for the sake of clarity, which is a measured spectrum taken at a backing pressure of 7 bars. The lower trace is calculated using the program PGOPHER⁴¹ with $T_{rot} = 3.5$ K.

TABLE I. The value of the detection parameters for SrF and BaF involved in the calculation of the number of molecules. Here, r and d correspond to the collection lens radius and the distance of the collection lens from the laser-induced fluorescence detection point, respectively.

Parameter	SrF	BaF
$S/pulse$	50	100
QE	0.39	0.13
T	0.73	0.35
n	5	1
Δy (mm)	10.4	10.4
w (mm)	1	1
r (mm)	12.7	25.4
d (mm)	27.3	65.7
Ω	1.17	0.42
M	1.7	0.5
$N/pulse$	10^4	6×10^5
$N/pulse/sr$	10^7	6×10^8

Substituting the detection parameter values for SrF and BaF from Table I into Eq. (4), we calculate that we have $\sim 6 \times 10^5$ BaF molecules per pulse and $\sim 1 \times 10^4$ SrF molecules per pulse in the $X^2\Sigma^+$ ($v = 0$, $N = 1$) state in the respective molecular beams after the skimmer accurate to within a factor of 2. The uncertainty on the molecule numbers is mostly due to the uncertainty on the numbers of photons scattered per molecule. The molecules per pulse per steradian can be calculated with respect to the nozzle exit, which is at a total distance of $R = 58$ cm from the LIF detection point.

The molecules per pulse is divided by a total factor of $4\pi(\Delta y/2)^2/R^2$ to give 6×10^8 and 1×10^7 BaF and SrF molecules per pulse per steradian in the $X^2\Sigma^+$ ($v = 0$, $N = 1$) state accurate to within a factor of 2, respectively. This state for BaF, like for SrF,^{45,46} can be laser cooled and Stark decelerated.

The observed difference in the density between BaF and SrF is surprising, given that barium and strontium are chemically very similar. The measurements on BaF were performed after the SrF measurements. We attribute the difference to the fact that we have put more effort in optimizing the BaF source than the SrF source. This difference is likely caused by differences in target ablation conditions, which were not completely optimized for SrF.

Furthermore, more barium metal ablation products seem to be entrained in the expanding carrier gas of the BaF molecular beam in comparison to the SrF beam at higher backing pressures. The barium ablation products add energy to the expanding gas, which is evident from an increase in the translational velocity of the BaF beam at high backing pressures in Fig 3.⁴⁷ The translational velocity of both BaF [604(4) m/s] and SrF [592(4) m/s] molecular beams is also larger than the velocity of the pure argon from a supersonic expansion (570 m/s) for a backing pressure of 5 bars. This fits with the higher density of BaF observed in the molecular beam in comparison to SrF.

Another possible explanation for the discrepancy in the molecule numbers between SrF and BaF may be due to the difference in the mass ratio of the molecule and the carrier gas. Heavier

molecules tend to bunch near the axis in supersonic expansion, which has been seen in the separation of gas mixtures.⁴⁸ A carrier gas with a different mass might change this discrepancy in the molecule number density of BaF and SrF.

IV. COMPARISON WITH OTHER WORK

Table II provides a comparison of the beam properties from this source to other ablation sources used to produce molecular beams of metal fluorides. The relative velocity ratio obtained in our case is lower than that reported for other sources.^{14,24,26} Two of these other BaF sources also produce beams with much higher rotational temperatures (20–50) K (see Table II) in comparison with our BaF source where we have achieved 3.5 K rotational temperature. The YbF source has a 3 K rotational temperature, which is comparable to the value obtained in our source.²⁴ The YbF source uses xenon as the carrier gas, while argon is used for all BaF sources. The beam intensity of SrF and BaF in this work also compares well with the intensity of the YbF source at a value of 1×10^9 molecules per steradian per pulse in a single rotational state. BaF beams have also been created using cryogenic buffer gas sources, resulting in beams with higher intensities in comparison with the beams from supersonic sources but with lower average velocity and larger velocity spread.^{50,51} A total of 3×10^{11} molecules per pulse have been produced for a beam of ThO molecules from a cryogenic source in the $X^1\Sigma^+$ ($v = 0$, $N = 0$) state.^{52,53}

V. OUTLOOK

We have demonstrated that with the combination of a pulsed gas beam from an Even–Lavie valve and laser ablation of metal atoms, beams of alkaline-earth monofluoride molecules can be produced with a low velocity spread and low rotational temperatures. The velocity spread achieved here is among the lowest measured for SrF and BaF. Despite the difference in the mass of SrF and BaF, the relative velocity spread achieved for these two molecules is similar and lower than the relative velocity spread for pure argon in a supersonic expansion. This shows that the molecular beam has completely thermalized with the carrier gas. It reaches the lower limit of motional temperature that can be achieved with this carrier gas. A similar velocity spread might be obtained for even heavier molecules.

TABLE II. Comparison of supersonic beam parameters for YbF, BaF, AlF, and SrF beams from different supersonic sources.

Molecule	Carrier gas (in K)	Rotational temperature (in K)	Relative velocity spread ($\Delta v/v$)
YbF ²⁴	Xe	3	0.082
BaF ²⁶	Ar	30	0.070
BaF ¹⁴	Ar	20–50	...
AlF ⁴⁹	Ar/Ne	10	...
BaF (this work)	Ar	3.5	0.054(9)
SrF (this work)	Ar	...	0.053(11)

ACKNOWLEDGMENTS

This work was done as part of the NL-eEDM collaboration, which receives funding (EEDM-166) from the Netherlands Organisation for Scientific Research (NWO).

DATA AVAILABILITY

The data that support the findings of this study are available from the corresponding author upon reasonable request.

REFERENCES

- G. Scoles, *Atomic and Molecular Beam Methods* (Oxford University Press, Oxford, NY, 1988).
- R. Campargue, *Atomic and Molecular Beams: The State of the Art 2000* (Springer-Verlag, Berlin, Heidelberg, 2001).
- R. E. Smalley, L. Wharton, and D. H. Levy, "The fluorescence excitation spectrum of rotationally cooled NO_2 ," *J. Chem. Phys.* **63**, 4977 (1975).
- J. Lim, J. R. Almond, M. R. Tarbutt, D. T. Nguyen, and T. C. Steimle, "The [557]- $X^2\Sigma^+$ and [561]- $X^2\Sigma^+$ bands of ytterbium fluoride, ^{174}YbF ," *J. Mol. Spectrosc.* **338**, 81–90 (2017).
- T. C. Steimle, S. Frey, A. Le, D. DeMille, D. A. Rahmlov, and C. Linton, "Molecular-beam optical Stark and Zeeman study of the $A^2\Pi-X^2\Sigma^+$ (0, 0) band system of BaF ," *Phys. Rev. A* **84**, 012508 (2011).
- M. Costes and C. Naulin, "Observation of quantum dynamical resonances in near cold inelastic collisions of astrophysical molecules," *Chem. Sci.* **7**, 2462–2469 (2016).
- I. W. M. Smith, "Reactions at very low temperatures: Gas kinetics at a new frontier," *Angew. Chem., Int. Ed.* **45**, 2842 (2006).
- H. L. Bethlem, G. Berden, and G. Meijer, "Decelerating neutral dipolar molecules," *Phys. Rev. Lett.* **83**, 1558–1561 (1999).
- S. Y. T. van de Meerakker, H. L. Bethlem, N. Vanhaecke, and G. Meijer, "Manipulation and control of molecular beams," *Chem. Rev.* **112**, 4828–4878 (2012).
- S. N. Vogels, Z. Gao, and S. Y. T. van de Meerakker, "Optimal beam sources for Stark decelerators in collision experiments: A tutorial review," *EPJ Tech. Instrum.* **2**, 12 (2015).
- J. Wang, V. A. Shamamian, B. R. Thomas, J. M. Wilkinson, J. Riley, C. F. Giese, and W. R. Gentry, "Speed ratios greater than 1000 and temperatures less than 1 mK in a pulsed He beam," *Phys. Rev. Lett.* **60**, 696–699 (1988).
- U. Even, J. Jortner, D. Noy, N. Lavie, and C. Cossart-Magos, "Cooling of large molecules below 1 K and He clusters formation," *J. Chem. Phys.* **112**, 8068 (2000).
- B. Yan, P. F. H. Claus, B. G. M. van Oorschot, L. Gerritsen, A. T. J. B. Eppink, S. Y. T. van de Meerakker, and D. H. Parker, "A new high intensity and short-pulse molecular beam valve," *Rev. Sci. Instrum.* **84**, 023102 (2013).
- A. Cournol, P. Pillet, H. Lignier, and D. Comparat, "Rovibrational optical pumping of a molecular beam," *Phys. Rev. A* **97**, 031401 (2018).
- T. G. Dietz, M. A. Duncan, D. E. Powers, and R. E. Smalley, "Laser production of supersonic metal cluster beams," *J. Chem. Phys.* **74**, 6511 (1981).
- D. E. Powers, S. G. Hansen, M. E. Geusic, A. C. Puij, J. B. Hopkins, T. G. Dietz, M. A. Duncan, P. R. R. Langridge-Smith, and R. E. Smalley, "Supersonic metal cluster beams: Laser photoionization studies of copper cluster Cu_2 ," *J. Phys. Chem.* **86**, 2556–2560 (1982).
- J. B. Hopkins, P. R. R. Langridge-Smith, M. D. Morse, and R. E. Smalley, "Supersonic metal cluster beams of refractory metals: Spectral investigations of ultracold Mo_2 ," *J. Chem. Phys.* **78**, 1627 (1983).
- G. Dorthe, M. Costes, C. Naulin, J. Jousset-Dubien, C. Vaucamps, and G. Nouchi, "Reactive scattering using pulsed crossed supersonic molecular beams. Example of the $\text{C} + \text{NO} \rightarrow \text{CN} + \text{O}$ and $\text{C} + \text{N}_2\text{O} \rightarrow \text{CN} + \text{NO}$ reactions," *Rev. Sci. Instrum.* **83**, 3171 (1985).
- M. Costes, C. Naulin, G. Dorthe, G. Daleau, J. Jousset-Dubien, C. Lalaude, M. Vinckert, A. Destor, C. Vaucamps, and G. Nouchi, "A pulsed crossed supersonic molecular beam apparatus to study the dynamics of refractory atom reactions," *J. Phys. E* **22**, 1017–1023 (1989).
- R. I. Kaiser and A. G. Suits, "A high-intensity, pulsed supersonic carbon source with $\text{C}(^3P_j)$ kinetic energies of 0.08–0.7 eV for crossed beam experiments," *Rev. Sci. Instrum.* **66**, 5405 (1995).
- T. C. Steimle, D. A. Fletcher, and C. T. Scurlock, "A molecular beam study of the (0, 0) $A^2\Pi-X^2\Sigma^+$ band system of SrF ," *J. Mol. Spectrosc.* **158**, 487–488 (1993).
- A. G. Adam, L. P. Fraser, W. D. Hamilton, and M. C. Steeves, "Gas-phase electronic spectroscopy of cobalt monofluoride," *Chem. Phys. Lett.* **230**, 82–86 (1994).
- D. A. Fletcher, K. Y. Jung, C. T. Scurlock, and T. C. Steimle, "Molecular beam pump/probe microwave-optical double resonance using a laser ablation source," *J. Chem. Phys.* **98**, 1837 (1993).
- M. R. Tarbutt, J. J. Hudson, B. E. Sauer, E. A. Hinds, V. A. Ryzhov, V. L. Ryabov, and V. F. Ezhov, "A jet beam source of cold YbF radicals," *J. Phys. B: At., Mol. Opt. Phys.* **35**, 5013 (2002).
- A. E. Leanhardt, J. L. Bohn, H. Loh, P. Maletinsky, E. R. Meyer, L. C. Sinclair, R. P. Stutz, and E. A. Cornell, "High-resolution spectroscopy on trapped molecular ions in rotating electric fields: A new approach for measuring the electron electric dipole moment," *J. Mol. Spectrosc.* **270**, 1–25 (2011).
- E. Altuntaş, J. Ammon, S. B. Cahn, and D. DeMille, "Measuring nuclear-spin-dependent parity violation with molecules: Experimental methods and analysis of systematic errors," *Phys. Rev. A* **97**, 042101 (2018).
- U. Even, "The Even-Lavie valve as a source for high intensity supersonic beam," *EPJ Tech. Instrum.* **2**, 17 (2015).
- C.-w. Dong, J.-x. Liu, F.-f. Li, and F.-y. Wang, "Laser ablation atomic beam apparatus with time-sliced velocity map imaging for studying state-to-state metal reaction dynamics," *Chin. J. Chem. Phys.* **29**, 99–104 (2016).
- D. Yan, Y.-j. Ma, F.-f. Li, J.-x. Liu, G.-j. Wang, and F.-y. Wang, "Imaging reaction dynamics of $\text{Y} + \text{SO}_2$," *Chin. J. Chem. Phys.* **33**, 239 (2020).
- N. Akerman, M. Karpov, Y. Segev, N. Bibelnik, J. Narevicius, and E. Narevicius, "Trapping of molecular oxygen together with lithium atoms," *Phys. Rev. Lett.* **119**, 073204 (2017).
- M. Karpov, M. Pitzer, Y. Segev, J. Narevicius, and E. Narevicius, "Low-energy collisions between carbon atoms and oxygen molecules in a magnetic trap," *New J. Phys.* **22**, 103055 (2020).
- R. Katzy, M. Singer, S. Izadnia, A. C. LaForge, and F. Stienkemeier, "Doping He droplets by laser ablation with a pulsed supersonic jet source," *Rev. Sci. Instrum.* **87**, 013105 (2016).
- The NL-eEDM Collaboration, P. Aggarwal, H. L. Bethlem, A. Borschevsky, M. Denis, K. Esajas, P. A. B. Haase, Y. Hao, S. Hoekstra, K. Jungmann, T. B. Meijknecht, M. C. Mooij, R. G. E. Timmermans, W. Ubachs, L. Willmann, and A. Zapara, "Measuring the electric dipole moment of the electron in BaF ," *Eur. Phys. J. D* **72**, 197 (2018).
- A. C. Vutha, M. Horbatsch, and E. A. Hessels, "Orientation-dependent hyperfine structure of polar molecules in a rare-gas matrix: A scheme for measuring the electron electric dipole moment," *Phys. Rev. A* **98**, 032513 (2018).
- P. Aggarwal, V. R. Marshall, H. L. Bethlem, A. Boeschoten, A. Borschevsky, M. Denis, K. Esajas, Y. Hao, S. Hoekstra, K. Jungmann, T. B. Meijknecht, M. C. Mooij, R. G. E. Timmermans, A. Touwen, W. Ubachs, S. M. Vermeulen, L. Willmann, Y. Yin, A. Zapara, and NL-eEDM Collaboration, "Lifetime measurements of the $A^2\Pi_{1/2}$ and $A^2\Pi_{3/2}$ states in BaF ," *Phys. Rev. A* **100**, 052503 (2019).
- J. B. Anderson and J. B. Fenn, "Velocity distributions in molecular beams from nozzle sources," *Phys. Fluids* **8**, 780 (1965).
- H. Haberland, U. Buck, and M. Tolle, "Velocity distribution of supersonic nozzle beams," *Rev. Sci. Instrum.* **56**, 1712 (1985).
- F. Reif, *Fundamentals of Statistical and Thermal Physics* (McGraw-Hill, Singapore, 1988).
- A. P. P. van der Poel, P. C. Zieger, S. Y. T. van de Meerakker, J. Loreau, A. van der Avoird, and H. L. Bethlem, "Cold collisions in a molecular synchrotron," *Phys. Rev. Lett.* **120**, 033402 (2018).
- A. P. P. van der Poel, "Cold collisions in a molecular synchrotron," Ph.D. thesis, Vrije Universiteit Amsterdam, 2018.

- ⁴¹C. M. Western, "PGOPHER: A program for simulating rotational, vibrational and electronic spectra," *J. Quant. Spectrosc. Radiat. Transfer* **186**, 221 (2017).
- ⁴²C. Effantin, A. Bernard, J. d'Incan, G. Wannous, J. Vergès, and R. F. Barrow, "Studies of the electronic states of the BaF molecule," *Mol. Phys.* **70**, 735–745 (1990).
- ⁴³J. F. Barry, "Laser cooling and slowing of a diatomic molecule," Ph.D. thesis, Yale University, 2013.
- ⁴⁴T. Chen, W. Bu, and B. Yan, "Structure, branching ratios, and a laser-cooling scheme for the ¹³⁸BaF molecule," *Phys. Rev. A* **94**, 063415 (2016).
- ⁴⁵E. S. Shuman, J. F. Barry, and D. DeMille, "Laser cooling of a diatomic molecule," *Nature* **467**, 820–823 (2010).
- ⁴⁶S. C. Mathavan, A. Zapara, Q. Esajas, and S. Hoekstra, "Deceleration of a supersonic beam of SrF molecules to 120 m/s," *ChemPhysChem* **17**, 3709–3713 (2016).
- ⁴⁷S. K. Tokunaga, J. O. Stack, J. J. Hudson, B. E. Sauer, E. A. Hinds, and M. R. Tarbutt, "A supersonic beam of cold lithium hydride molecules," *J. Chem. Phys.* **126**, 124314 (2007).
- ⁴⁸P. C. Waterman and S. A. Stern, "Separation of gas mixtures in a supersonic jet," *J. Chem. Phys.* **31**, 405 (1959).
- ⁴⁹S. Truppe, S. Marx, S. Kray, M. Doppelbauer, S. Hofsäss, H. C. Schewe, N. Walter, J. Pérez-Ríos, B. G. Sartakov, and G. Meijer, "Spectroscopic characterization of aluminum monofluoride with relevance to laser cooling and trapping," *Phys. Rev. A* **100**, 052513 (2019).
- ⁵⁰W. Bu, T. Chen, G. Lv, and B. Yan, "Cold collision and high-resolution spectroscopy of buffer-gas-cooled BaF molecules," *Phys. Rev. A* **95**, 032701 (2017).
- ⁵¹R. Albrecht, M. Scharwaechter, T. Sixt, L. Hofer, and T. Langen, "Buffer-gas cooling, high-resolution spectroscopy, and optical cycling of barium monofluoride molecules," *Phys. Rev. A* **101**, 013413 (2020).
- ⁵²N. R. Hutzler, H.-I. Lu, and J. M. Doyle, "The buffer gas source: An intense, cold, and slow source for atoms and molecules," *Chem. Rev.* **112**, 4803–4827 (2012).
- ⁵³N. R. Hutzler, "A new limit on the electron electric dipole moment: Beam production, data interpretation and systematics," Ph.D. thesis, Harvard University, 2014.